



# Endocast morphology of *Homo naledi* from the Dinaledi Chamber, South Africa

Ralph L. Holloway<sup>a,1,2</sup>, Shawn D. Hurst<sup>b,1</sup>, Heather M. Garvin<sup>c,d</sup>, P. Thomas Schoenemann<sup>b,e</sup>, William B. Vanti<sup>f</sup>, Lee R. Berger<sup>d</sup>, and John Hawks<sup>d,g,2</sup>

<sup>a</sup>Department of Anthropology, Columbia University, New York, NY 10027; <sup>b</sup>Department of Anthropology, Indiana University, Bloomington, IN 47405; <sup>c</sup>Department of Anatomy, Des Moines University, Des Moines, IA 50312; <sup>d</sup>Evolutionary Studies Institute, University of Witwatersrand, Johannesburg 2000, South Africa; <sup>e</sup>Stone Age Institute, Bloomington, IN 47405; <sup>f</sup>Science and Engineering Library, Columbia University, New York, NY 10027; and <sup>g</sup>Department of Anthropology, University of Wisconsin–Madison, Madison, WI 53706

Contributed by Ralph L. Holloway, April 5, 2018 (sent for review December 1, 2017; reviewed by James K. Rilling and Chet C. Sherwood)

**Hominin cranial remains from the Dinaledi Chamber, South Africa, represent multiple individuals of the species *Homo naledi*. This species exhibits a small endocranial volume comparable to *Australopithecus*, combined with several aspects of external cranial anatomy similar to larger-brained species of *Homo* such as *Homo habilis* and *Homo erectus*. Here, we describe the endocast anatomy of this recently discovered species. Despite the small size of the *H. naledi* endocasts, they share several aspects of structure in common with other species of *Homo*, not found in other hominins or great apes, notably in the organization of the inferior frontal and lateral orbital gyri. The presence of such structural innovations in a small-brained hominin may have relevance to behavioral evolution within the genus *Homo*.**

brain evolution | human evolution | South Africa | *Homo* | paleoanthropology

Human brains are larger than those of the living great apes, and they also exhibit many differences in organization from those primates. Understanding when and how these changes took place is the key challenge of paleoneurology (1, 2). The size of the brain and several externally visible aspects of brain anatomy can be assessed in fossil hominins based upon evidence from endocasts, which are natural or artificial impressions of the endocranial surface. Endocasts do not perfectly reflect the underlying cerebral cortex, in part because three tissue layers separate the endocranial surface from the brain itself and in part because many fossils present insufficient surface detail to preserve clear evidence of gyral and sulcal impressions. Nevertheless, some endocasts provide enough sulcal morphology to enable reliable identification of features with salience for functional interpretations (1–5).

Hominin skeletal material from the Dinaledi Chamber, South Africa, represents the species *Homo naledi* (6). This fossil assemblage represents at least 15 individuals, both adults and juveniles across all stages of development (7). The Dinaledi Chamber assemblage was deposited between 236,000 and 335,000 y ago (8), meaning that this sample of *H. naledi* existed at the same time as some archaic humans within Africa (9), including those that some workers identify as “early *Homo sapiens*” (10). The cranial, dental, and postcranial remains of *H. naledi* exhibit a mosaic of derived, humanlike traits combined with primitive traits shared with *Australopithecus* and other stem hominins (6, 11). This morphological pattern makes it difficult to determine the phylogenetic placement of *H. naledi* relative to other species within *Homo*: For example, Bayes factor tests on cranial and dental traits clearly place *H. naledi* within the *Homo* clade, but do not exclude it as a sister taxon of *Homo antecessor*, Asian *Homo erectus*, *Homo floresiensis*, *Homo habilis*, or even *H. sapiens* (12). The small endocranial volume (ECV) of *H. naledi*, which is within the range known for australopithecids, is one of many primitive traits that contrast with other, more humanlike, cranial and dental traits.

We examined the endocast morphology of *H. naledi* from the Dinaledi Chamber and compared this morphology with other hominoids and fossil hominins. The skeletal material from the Dinaledi Chamber includes seven cranial portions that preserve substantial endocranial surface detail, representing partial crania of at least five individuals. The external morphology of these specimens has been described and illustrated (13). All are morphologically consistent with an adult developmental stage. Collectively, the remains document nearly the entire cortical surface (*SI Appendix*, Fig. S1) with a high degree of gyral and sulcal detail. The DH1 calvaria preserves portions of the left and right parietal lobes, complete left and mostly complete right occipital lobes, and a small portion of both cerebellar lobes. The endocranial surface of the DH3 calvaria preserves a mostly complete left hemisphere with most of the frontal, temporal, and parietal lobes. Additional fragments, including the DH2 and DH4 calvariae, duplicate some of this morphology and in no case contradict the morphology observable in the relatively more complete specimens.

The DH1 (Fig. 1 and *SI Appendix*, Fig. S2) and DH2 (*SI Appendix*, Figs. S3 and S4) calvariae represent individuals with approximately the same ECV, while the DH3 (Fig. 2 and *SI Appendix*, Fig. S5) calvaria is smaller. Previously, virtual reconstruction of these crania yielded volume estimates of 560 mL for a composite model based on DH1 and DH2 elements and 465 mL for the DH3/DH4 composite (6). Here, we have carried out physical reconstructions of the DH1 and DH3 specimens (*SI*

## Significance

The new species *Homo naledi* was discovered in 2013 in a remote cave chamber of the Rising Star cave system, South Africa. This species survived until between 226,000 and 335,000 y ago, placing it in continental Africa at the same time as the early ancestors of modern humans were arising. Yet, *H. naledi* was strikingly primitive in many aspects of its anatomy, including the small size of its brain. Here, we have provided a description of endocast anatomy of this primitive species. Despite its small brain size, *H. naledi* shared some aspects of human brain organization, suggesting that innovations in brain structure were ancestral within the genus *Homo*.

Author contributions: R.L.H., S.D.H., H.M.G., P.T.S., W.B.V., L.R.B., and J.H. designed research, performed research, analyzed data, and wrote the paper.

Reviewers: J.K.R., Emory University; and C.C.S., George Washington University.

Conflict of interest statement: R.L.H. and C.C.S. are coauthors on a 2018 paper published in PNAS.

This open access article is distributed under Creative Commons Attribution-NonCommercial-NoDerivatives License 4.0 (CC BY-NC-ND).

<sup>1</sup>R.L.H. and S.D.H. contributed equally to this work.

<sup>2</sup>To whom correspondence may be addressed. Email: Rlh2@columbia.edu or jhawks@wisc.edu.

This article contains supporting information online at [www.pnas.org/lookup/suppl/doi:10.1073/pnas.1720842115/-DCSupplemental](http://www.pnas.org/lookup/suppl/doi:10.1073/pnas.1720842115/-DCSupplemental).

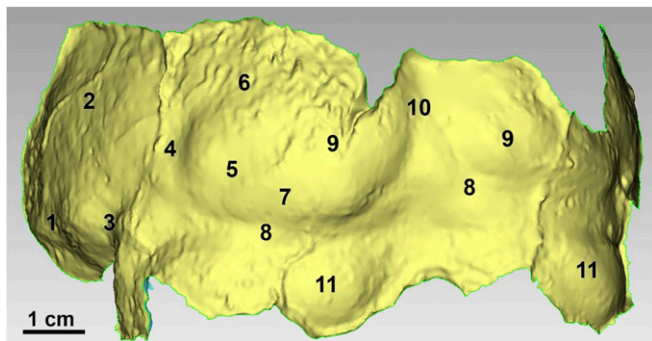


**Fig. 1.** Posterior oblique view of 3D model of the positive endocranial surface of the DH1 occipital fragment with oblique lighting applied and features labeled: 1, temporo-occipital fissure; 2, parietal lobe; 3, beginning of sigmoid sulcus; 4, possible lunate sulcus; 5, inferior occipital sulcus; 6, possible dorsal remnant of the lunate sulcus; 7, possible occipital polar sulcus; 8, transverse sinus; 9, occipital pole; 10, midsagittal plane; and 11, cerebellar lobe.

*Appendix*), resulting in water-displacement volumes of 555 mL for DH1 and 460 mL for DH3, both in good agreement with the virtual reconstructions.

The most notable morphological differences of the frontal lobes between humans and apes involve the inferior frontal and lateral orbital gyri. In apes, this area of the frontal lobes includes the fronto-orbital sulcus, which is usually well preserved on ape endocasts. A fronto-orbital sulcus is also evident on the MH1 endocast of *Australopithecus sediba* (14) and on some endocasts of *Australopithecus africanus* (15, 16). In humans, a fronto-orbital sulcus is not apparent on the external surface of the cortex. Instead, posterior and ventral expansion of the frontal lobes has caused the human inferior frontal and lateral orbital gyri to cover over, or operculate, the anterior area of the insula, forming the frontal opercula; these are divided by the vertical and horizontal rami of the lateral fissure (refs. 17–19, Fig. 3, and *SI Appendix*, Figs. S6 and S7). Together, these define the borders (*SI Appendix*, Fig. S8) of the frontal operculum or *pars triangularis* (associated with Brodmann area 45). Just inferior to the *pars triangularis* is the orbital operculum or *pars orbitalis* (associated with Brodmann area 47). Just caudal to both is the fronto-parietal operculum or *pars opercularis* (associated with Brodmann area 44).

Many endocasts of Plio-Pleistocene *Homo* lack convolutional detail in this region. A humanlike frontal operculum is clearly visible on some specimens of *H. erectus* and on endocasts from the Sima de los Huesos, which represent early members of the Neanderthal lineage (3, 4, 20). No evidence of an ancestral fronto-orbital sulcus can be seen on either KNM-ER 1470 (*Homo rudolfensis*) or OH 16 (*H. habilis*) (21, 22). KNM-ER 1470 has been argued to have a derived configuration with vertical and horizontal rami of the lateral fissure (21), although this is not visible to us on that endocast.

The DH3 endocast of *H. naledi* has no fronto-orbital sulcus, similar to *Homo* and different from apes and *Australopithecus*. A vertical ramus of the lateral fissure as well as a horizontal branch off this (Fig. 3 and *SI Appendix*, Figs. S5 and S9) permits a clear identification of a derived frontal operculum in this endocast (23). DH3 displays a Y-shaped pattern of sulcal separation, found in between one-fourth to one-third of modern human hemispheres (17, 24). The inferior portion of the convolution suggests a very pronounced *pars orbitalis*, while the *pars triangularis* is slight, similar to the condition Falk (21) suggested for KNM-ER 1470. DH3 is the smallest endocast where this humanlike morphological pattern is clearly preserved. DH3 also has particularly clear middle and inferior frontal sulci that

parallel each other. The entire frontal bends sharply in an anterior–inferior direction toward the ventral edge (*SI Appendix*, Fig. S5), rather than more directly anteriorly toward the frontal pole, which is also a derived trait (18).

Hominin endocasts differ from great apes in the extent of frontal and occipital petalial asymmetry (25, 26). None of the endocasts of *H. naledi* from the Dinaledi Chamber preserve both frontal poles and lateral prefrontal surfaces, preventing an assessment of frontal petalia. The left frontal pole of DH3 suggests a somewhat greater lateral width. The DH1 occipital shows a left occipital petalia, with the left occipital lobe both markedly larger and more posteriorly projecting than the right (Fig. 1). U.W. 101–200 is a less complete occipital fragment but is consistent with a left occipital petalia equally marked as DH1 (*SI Appendix*, Fig. S12). This pattern is commonly seen in modern humans and fossil hominins, including both *Homo* and *Australopithecus*, although the greater degree of petalial asymmetry seen in *H. naledi* is most like that seen in modern humans and the larger fossil endocasts of later *Homo*. Greater variation in asymmetry within the human brain has been suggested to reflect a degree of adaptive plasticity than other living primates (27). In modern humans, left occipital petalia with right frontal petalia is associated with righthandedness (28).

One indicator of the posterior organization of the brain is the position of the lunate sulcus. This sulcus is relatively well-marked in many endocasts of great apes, where its high, transversely extensive and relatively rostral position marks the extent of the primary visual cortex. In living humans, the overall cortex is substantially larger, but the primary visual cortex is relatively less enlarged than the cortex as a whole. The lunate sulcus in humans is variable and less well represented on the cortical surface, but

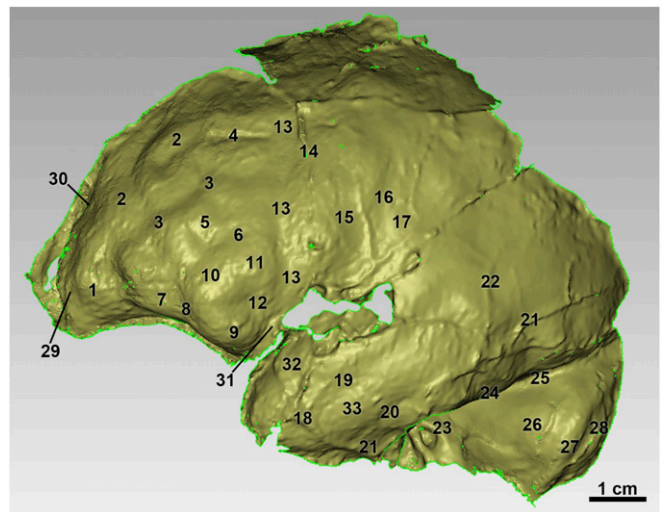


**Fig. 2.** Lateral view of 3D model of the positive endocranial surface of the DH3 fragment with oblique lighting applied and features labeled: 1, gyrus rectus; 2, middle frontal gyrus superior part; 3, middle frontal sulcus; 4, artifact; 5, middle frontal gyrus inferior part; 6, inferior frontal sulcus; 7, lateral orbital gyrus; 8, possible lateral orbital sulcus; 9, inferior frontal gyrus (*pars orbitalis*, Brodmann area 47); 10, inferior frontal gyrus (*pars triangularis*, Brodmann area 45); 11, inferior frontal gyrus (*pars opercularis*, Brodmann area 44); 12, vertical ramus of the lateral fissure, with horizontal branch; 13, precentral sulcus; 14, remnant coronal suture; 15, precentral gyrus; 16, central sulcus; 17, postcentral gyrus; 18, anterior branch of middle meningeal; 19, superior temporal sulcus; 20, middle temporal sulcus; 21, posterior branch of middle meningeal; 22, middle branch of middle meningeal; 23, internal auditory meatus; 24, temporal/cerebellar cleft; 25, temporo-occipital incisure; 26, anterior lobe of cerebellum; 27, sigmoid sulcus; 28, posterior lobe of cerebellum; 29, frontal pole; 30, midsagittal plane; 31, lateral fissure; 32, superior temporal gyrus; and 33, middle temporal gyrus.

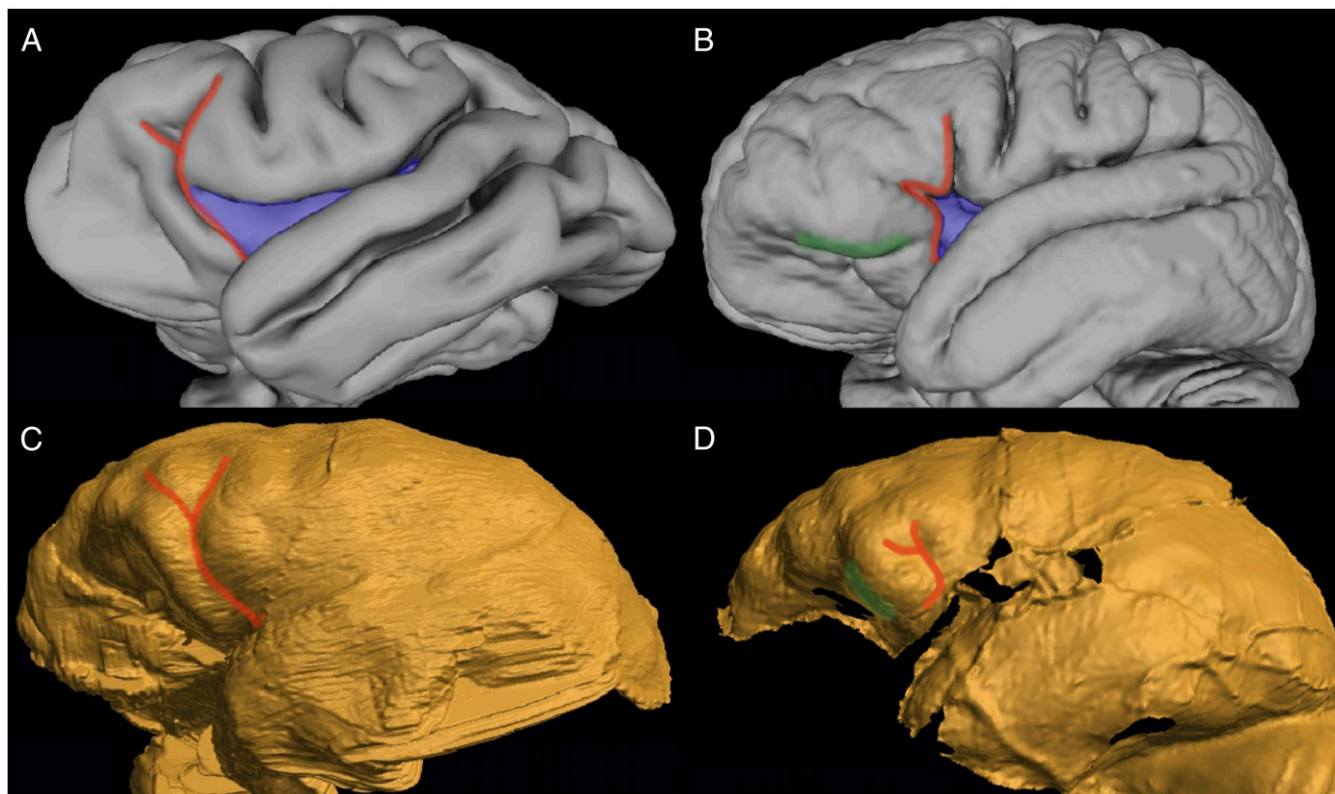


**Fig. 3.** Evolution of the inferior frontal gyrus. (A) *P. troglodytes* (ISIS 6167) brain “Bria” (27). (B) *H. sapiens* 152-subject averaged brain. (C) *Au. sediba* MH1 endocast. (D) *H. naledi* DH3 endocast. See *Materials and Methods* for provenance of these models. In the ancestral condition seen in A, the anterior area of the deep insula (purple) is exposed, while the posterior area is covered over by the parietal and temporal lobes (which meet to form the lateral fissure). The fronto-orbital sulcus with a horizontal branch (dark red) lies directly anterior and medial to the insula, on the orbital surface of the brain. (B) In *H. sapiens*, the frontal lobe has expanded posteriorly and ventrally (*SI Appendix, Figs. S6 and S7*), causing the anterior insula to be covered over, similarly to the posterior insula. Here, the vertical ramus of the lateral fissure with its horizontal branch (dark red) is the external homolog of the superior part of the fronto-orbital sulcus, while the basal segment of the lateral fissure is the external homolog of the inferior part. The buried anterior limiting sulcus of the insula (*SI Appendix, Fig. S6*) is the internal homolog of the inferior fronto-orbital sulcus. (C and D) In *Au. sediba* (C) the fronto-orbital sulcus is in the ancestral condition, but thickening of the orbital surface just anterior to this suggests an intermediate condition between other australopithecines and later *Homo* (14, 23); in *H. naledi* (D), the presence of a vertical ramus of the lateral fissure with horizontal branch and thickened orbital area immediately anterior and ventral to this suggest frontal lobe expansion and fully derived inferior frontal gyrus morphology (23).

when it occurs is less extensive and more posteriorly positioned than in apes. The relatively greater expansion of association cortical areas compared with primary visual cortex is notable in human brain evolution, but the identification of the lunate sulcus in endocasts of fossil hominins is difficult and has been historically controversial (1, 2).

The DH1 endocast bears faint traces of a lateral remnant of the lunate sulcus on the left side and of a dorsal bounding lunate as well (no. 6 in Fig. 1). The right side of this endocast shows a very small groove at the end of the lateral sinus, which could be a remnant of the lunate sulcus. The width from the left lateral lunate impression to the midline is ~43 mm. This measure is significantly less ( $P < 0.001$ ) than found in a sample of 75 chimpanzee (*Pan troglodytes*) hemispheres (refs. 29 and 30 and *SI Appendix, Table S1*), despite the larger ECV of DH1 (560 mL) in comparison with chimpanzees. Neither the DH4 endocast remnant (Fig. 4 and *SI Appendix, Fig. S10*) nor the U.W. 101-770 occipital fragment (*SI Appendix, Fig. S11*) bear any sign of a lunate sulcus, but U.W. 101-200 may preserve a dorsal portion of it (landmark 1; *SI Appendix, Fig. S12*). Based on these observations, we suggest that *H. naledi* retained a lunate sulcus that was smaller in extent than in chimpanzees and that the dorsal remnant of the lunate is comparatively reduced. In our assessment, this is compatible with morphology present in endocasts of both *Homo* and *Australopithecus*.

## Discussion

The endocranial form of *H. naledi* shares aspects of cortical organization with endocasts of *H. habilis*, *H. rudolfensis*, *H. floresiensis*, and *H. erectus*. We hypothesize that these shared derived endocast features, particularly in the inferior frontal and lateral orbital gyri, were present in the last common ancestor of *Homo*. The ancestor of *Homo* would thus have been different from *Au. sediba* and *Au. africanus* in such endocast features (14–16), although *Au. sediba* (Fig. 3 and *SI Appendix, Fig. S7*) might have represented an intermediate condition (14, 23).

Despite these similarities of form, species of *Homo* differ greatly in brain size. *H. naledi* and *H. floresiensis* had small volumes within or just above the range of *Australopithecus* (11, 31). Specimens attributed to *H. habilis* range from 500 to >700 mL (22, 32), and *H. rudolfensis* includes two specimens of 752 and 830 mL (33). *H. erectus*, if it is defined to include both the Dmanisi and Ngandong hominin samples, exhibits a striking range of ECV from 550 to >1,200 mL (33, 34). However, regardless of size, each of these species shares similar frontal lobe morphology, even those with brain size within the range of *Australopithecus* samples. The form of the frontal lobes was not simply an allometric consequence of larger brain size in *Homo*. The extensive occipital petalial asymmetry in DH1 is similar to later, larger-brained species of *Homo* and may likewise suggest that this trait is not merely a consequence of larger brain size.

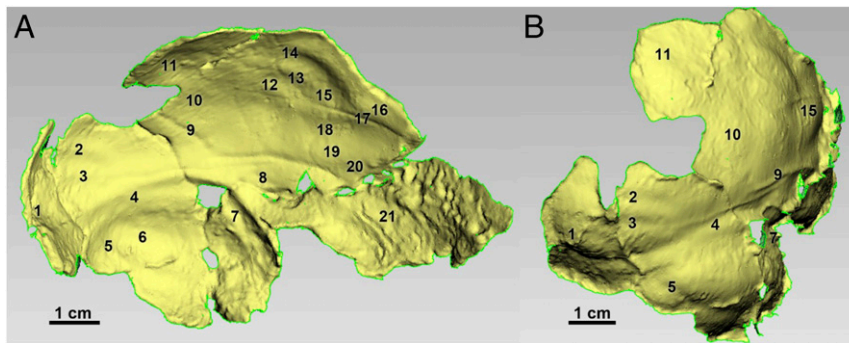


**Fig. 4.** Lateral oblique (A) and posterior oblique (B) view of 3D model of the positive endocranial surface of the DH4 fragment with oblique lighting and features labeled; 1, occipital pole; 2, lateral occipital sulcus; 3, inferior occipital sulcus; 4, transverse sinus; 5, great cerebellar sulcus; 6, cerebellum; 7, sigmoid sinus; 8, middle temporal gyrus; 9, posterior branch of middle meningeal; 10, part of angular gyrus; 11, part of supramarginal gyrus; 12, postcentral sulcus; 13, posterior subcentral sulcus; 14, central sulcus; 15, postcentral gyrus; 16, precentral gyrus; 17, anterior branch of middle meningeal; 18, lateral fissure; 19, superior temporal gyrus; 20, superior temporal sulcus; and 21, surface of petrosquamous suture.

The morphological characters that distinguish the frontal cortex of *Homo* from known endocasts of *Australopithecus* have been implicated in the evolution of tool use, language, and social behavior. It has been suggested that *pars opercularis* and *pars triangularis*, which involve Brodmann areas 44 and 45, function in the planning of motor sequences underlying Oldowan tool production in addition to the production of speech (35), although the degree to which this is true has been disputed (36). The *pars orbitalis*, which involves Brodmann's area 47, is associated with language processing (37) and the recognition and production of social emotions, social inhibition, and emotional learning (38); it also differs in organization between hominoids (23). Additionally, a shift toward more extensive occipital petalial asymmetry has been implicated in the evolution of language abilities in the human lineage. The ubiquity of such features within *Homo*, including the small-brained *H. naledi*, suggests that a behavioral niche with serialized communication, planning, and complex action sequences that underlie tool production, as well as increased display of prosocial emotions, may have been the environment for natural selection during the evolution of *Homo*, even for species like *H. naledi* that lack the substantial increases in overall brain size evident in archaic humans and modern *H. sapiens*.

The geological age of the Dinaledi Chamber sample of *H. naledi*, between 236,000 and 335,000 y ago (8), prompts the question of whether its small brain size was a retention from the common ancestor of *Homo*, possibly >2 Mya, or whether the small brain size of *H. naledi* may instead have resulted from secondary reduction from a later, larger-brained form of *Homo* (13). In our interpretation, the derived aspects of endocranial morphology in *H. naledi* were likely present in the common ancestor of the genus and do not by themselves provide evidence of close relationship between *H. naledi* and *H. sapiens* or other, larger-brained species within *Homo*. These morphological observations therefore provide no new evidence to test a possible evolutionary reversal or reduction in brain size in this species. To test whether small brain size was retained in *H. naledi* from the common ancestor of *Homo*, or whether instead small brain size evolved secondarily in this lineage, will require better resolution of the phylogenetic tree connecting it to other species of *Homo*. In the case of *H. floresiensis*, a similar question has arisen: Once considered as a possible dwarfed descendant of *H. erectus* (39), recent phylogenetic comparisons suggest that *H. floresiensis* may have branched from a more basal node of the *Homo* phylogeny (40, 41). *H. naledi* does not appear to be closely related to *H. floresiensis*, and the two share different suites of features with more derived species within *Homo* (11), so while these two cases may look similar in presenting small brain size in late-surviving

species of *Homo*, we are not prepared to draw any independent conclusion about the relationships or validity of *H. floresiensis* without further study. *H. naledi* adds further evidence that the evolution of brain size in *Homo* was diverse and was not a simple pattern of gradual increase over time.

In recent years, anthropologists have begun to reassess the adaptive importance of brain size. Brain size was once commonly viewed as one of the most important distinguishing features of the genus *Homo* (42). Many hypothesized that the evolution of larger brains was correlated with the evolution of smaller postcanine teeth, as *Homo* pursued a dietary strategy relying upon higher-energy foods and tool use to increase caloric return and fuel a larger brain (43, 44). However, a broader comparison shows that brain size and shape, and postcanine tooth size and shape, were not phylogenetically correlated in hominins (45). Furthermore, *H. naledi*, *H. floresiensis*, and *Au. sediba* all exhibit smaller postcanine dentitions and smaller brain sizes than *H. habilis* and *H. erectus* (6, 11, 14, 31, 39). *H. naledi* in particular shares derived hand and wrist morphology, and lower limb and foot morphology, with humans and Neanderthals (many of these features are not represented in known *H. erectus* fossils) that suggest humanlike abilities to manipulate objects and use landscapes (6, 9, 46–49).

As shown here, structural information from endocasts suggests that small and large brains within *Homo* shared many aspects of organization. Behaviors including stone tool manufacture, sociality, and foraging that are shared across the genus *Homo* may have selected for such a pattern of brain organization. Increases in overall brain size occurred in one or more lineages of *Homo* and may reflect specific aspects of adaptive pattern in these lineages. Brain size evolution was not a unitary trend in human ancestry, and we must work to understand a more complex pattern. Future work on the hominin fossil material attributed to *H. naledi* from the Lesedi Chamber (11), including the LES1 cranium, may test these hypotheses and provide additional information about endocast morphology in this species.

## Materials and Methods

All Dinaledi fossil material is available for study by researchers upon application to the Evolutionary Studies Institute at the University of the Witwatersrand where the material is curated (contact Bernhard Zipfel). Surface scans of the Dinaledi cranial fragments were created by using a NextEngine Desktop laser scanner (model 2020i). Between 8 and 12 divisions were used depending on the fragment and were scanned at the highest standard-definition setting. These 8–12 scans were then merged in the accompanying ScanStudio HD Pro software. Two 360-degree scans were completed for each fragment. These 360-degree scans were then aligned and merged in Geomagic Studio (Version 2014.1.0; Raindrop Geomagic) to create a complete 3D model of the fragment. Dinaledi 3D surface and other digital data are

available from the MorphoSource digital repository ([morphosource.org/index.php/Detail/ProjectDetail/Show/project\\_id/124](http://morphosource.org/index.php/Detail/ProjectDetail/Show/project_id/124)).

The ectocranial surfaces of each cranial fragment 3D model were manually deleted to reveal the “positive” model of the endocranial surface that corresponds with cortical morphology. Different orientations, object colors, lighting, reflectivity settings, and curvature maps were then used within GeoMAGIC Studio to better illustrate the endocranial features. This was done consistently within each image; in this regard, no area was digitally enhanced compared with the others. Endocranial descriptions were based on these digital models as well as physical models created from them with a Zortrax model M200 3D printer and/or with silicon molding material (Dentsply and Equinox) used on the endocranial surfaces of the 3D prints. These models were then compared with 35 chimpanzee endocasts, 10 chimpanzee brain casts, 5 fixed chimpanzee brains, a digital brain model averaged from 29 chimpanzee MRIs, 14 human hemisphere endocasts, 5 fixed human brains, and a digital brain model averaged from 152 human MRIs.

The 3D surface data of the MH1 endocast (14) were acquired from the Evolutionary Studies Institute at the University of the Witwatersrand. The 3D surface data of the “Bria” (ISIS 6167) chimpanzee brain (27) were acquired from the National Chimpanzee Brain Resource ([www.chimpanzeebrain.org](http://www.chimpanzeebrain.org)). The 3D surface data of the 29-subject averaged chimpanzee brain were acquired from the Van Essen laboratory at Washington University in St. Louis. The 3D surface data of the MNI 152 averaged human brain were acquired from the Montreal Neurological Institute ([www.mcgill.ca/neuro](http://www.mcgill.ca/neuro)). While we have atlases of human and chimpanzee cortical morphology, there are no atlases for their last common ancestor or for early hominins. Consequently, our identifications were based on both modern ape and modern human cortical maps and available cytoarchitectonic maps (18, 19, 50–52).

In the original report (6), two ECVs were provided by using virtual composites of the DH3/DH4 and DH1/DH2 fragments. Missing portions and the cranial bases were closed virtually by using a “Fill by Curvature” hole-filling function. The resultant ECV values were 465 cm<sup>3</sup> (DH3/DH4) and 560 cm<sup>3</sup> (DH1/DH2). When the basal endocranial portion of STS 19 *Au. africanus* specimen was scaled and fit to the smaller DH3/DH4 composite to better simulate the cranial base form, the ECV estimate did not change significantly.

In this study, we 3D-printed original composite models (without the missing basal portions) and made manual endocast reconstructions, using plasticine to provide the missing basal portions (rostral bec, temporal lobe poles, clivus, cerebellar lobes, and foramen magnum) on the 3D prints. To do so, the basal portions of the 3D prints were flattened by the printing process and were cut away to the edges of the actual endocranial portions, exposing the honeycomb matrix formed during the printing process. These were filled with plaster so that the reconstructions would not float during water immersion for volume estimation. Plasticine was modeled to effect reasonable imitations of the missing portions, based on comparative specimens. The models were then immersed in water, and the water displacement was documented as the volume. The smaller ECV value was 460 mL, and the larger ECV value was 555 mL, each being the average of three measurements. These reconstructions (SI Appendix, Fig. S13) were within 5 mL of the original estimates, thus confirming the ECVs originally published.

**ACKNOWLEDGMENTS.** The specimens of *H. naledi* described in this study are curated in the Evolutionary Studies Institute at the University of the Witwatersrand. The 3D surface data of the Dinaledi fossil material are available from [Morphosource.org](http://Morphosource.org). The 3D surface data of the MH1 endocast are curated in the Evolutionary Studies Institute at the University of the Witwatersrand. The 3D surface data of the “Bria” (ISIS 6167) chimpanzee brain are courtesy of Aida Gomez Robles and Chet Sherwood and are curated at the National Chimpanzee Brain Resource (supported by NIH Grant NS092988). The 3D surface data of the 29-subject averaged chimpanzee brain were acquired from the Van Essen laboratory at Washington University in St. Louis and are courtesy of Matthew Glasser and David Van Essen of Washington University in St. Louis and James Rilling and Todd Preuss of Emory University. The 3D surface data of the MNI 152 averaged human brain were courtesy of the Montreal Neurological Institute. This work was supported by the National Geographic Society, the National Research Foundation of South Africa, the Lyda Hill Foundation, the Fulbright Scholar Program, the Vilas Trust, and the Wisconsin Alumni Research Foundation. P.T.S. was supported by Grant 52935 from the John Templeton Foundation titled “What Drives Human Cognitive Evolution?” (N. Toth, K. Schick, C. Allen, P. Todd, and P.T.S., coprincipal investigators).

- Holloway RL, Sherwood CC, Hof PR, Rilling JK (2009) Evolution of the brain in humans–Paleoneurology. *Encyclopedia of Neuroscience* (Springer, Berlin), pp 1326–1334.
- Falk D, et al. (2000) Early hominid brain evolution: A new look at old endocasts. *J Hum Evol* 38:695–717.
- Dubois E (1933) The shape and size of the brain in *Sinanthropus* and in *Pithecanthropus*. *Proc R Acad Amsterdam* 36:415–423.
- Kappers C, Bouman K (1939) Comparison of the endocranial casts of the *Pithecanthropus erectus* skull found by Dubois and von Koenigswald's *Pithecanthropus* skull. *K Ned Akad Wet* 42:30–40.
- Dart RA (1929) *Australopithecus africanus; and His Place in Human Origins* (University of Witwatersrand Archives, Johannesburg).
- Berger LR, et al. (2015) *Homo naledi*, a new species of the genus *Homo* from the Dinaledi Chamber, South Africa. *eLife* 4:e09560.
- Bolter D, Bogin B, Cameron N, Hawks J (2017) Palaeodemographics of individuals in the Dinaledi Chamber using dental remains. *S Afr J Sci* 114:2017-0066.
- Dirks PH, et al. (2017) The age of *Homo naledi* and associated sediments in the Rising Star Cave, South Africa. *eLife* 6:e24231.
- Berger LR, Hawks J, Dirks PH, Elliott M, Roberts EM (2017) *Homo naledi* and Pleistocene hominin evolution in subequatorial Africa. *eLife* 6:e24234.
- Hublin JJ, et al. (2017) New fossils from Jebel Irhoud (Morocco) and the Pan-African origin of *Homo sapiens*. *Nature* 546:289–292.
- Hawks J, et al. (2017) New fossil remains of *Homo naledi* from the Lesedi Chamber, South Africa. *eLife* 6:e24232.
- Dembo M, et al. (2016) The evolutionary relationships and age of *Homo naledi*: An assessment using dated Bayesian phylogenetic methods. *J Hum Evol* 97:17–26.
- Laird MF, et al. (2017) The skull of *Homo naledi*. *J Hum Evol* 104:100–123.
- Carlson KJ, et al. (2011) The endocast of MH1, *Australopithecus sediba*. *Science* 333:1402–1407.
- Schepers GWH (1946) The endocranial casts of the South African ape-man. Part 2. *The South African Fossil Ape Men, The Australopithecines*, Memoir 2 (Transvaal Museum, Pretoria, South Africa).
- Schepers GWH (1950) The brains casts of the recently discovered Plesianthropus skulls. Part II. *Sterkfontein Ape-Man Plesianthropus*, Memoir 4, eds Broom R, Robinson JT, Schepers GWH (Transvaal Museum, Pretoria, South Africa).
- Cunningham D, Horsley V (1892) *Contribution to the Surface Anatomy of the Cerebral Hemispheres* (Academy House, Dublin).
- Connolly CJ (1950) *External Morphology of the Primate Brain* (C. C Thomas, Springfield, IL), p xiii.
- Duvernoy H (1991) *The Human Brain* (Springer, New York).
- Poza-Rey EM, Lozano M, Arsuaga JL (2017) Brain asymmetries and handedness in the specimens from the Sima de los Huesos site (Atapuerca, Spain). *Quat Int* 433:32–44.
- Falk D (1983) Cerebral cortices of East African early hominids. *Science* 221:1072–1074.
- Tobias PV (1987) The brain of *Homo habilis*: A new level of organization in cerebral evolution. *J Hum Evol* 16:741–761.
- Hurst SD (2017) Emotional evolution in the frontal lobes: Social affect and lateral orbitofrontal cortex morphology in hominoids. PhD dissertation (Indiana University, Bloomington, IN).
- Iidow OE, Soyemi S, Atobatele K (2014) Morphometry, asymmetry and variations of the sylvian fissure and sulci bordering and within the pars triangularis and pars operculum: An autopsy study. *J Clin Diagn Res* 8:AC11–AC14.
- Holloway RL, De La Costelareymondie MC (1982) Brain endocast asymmetry in pongids and hominids: Some preliminary findings on the paleontology of cerebral dominance. *Am J Phys Anthropol* 58:101–110.
- Balzeau A, Gilissen E, Grimaud-Hervé D (2012) Shared pattern of endocranial shape asymmetries among great apes, anatomically modern humans, and fossil hominins. *PLoS One* 7:e29581.
- Gómez-Robles A, Hopkins WD, Sherwood CC (2013) Increased morphological asymmetry, evolvability and plasticity in human brain evolution. *Proc Biol Sci* 280:20130575.
- Hervé PY, Crivello F, Perchey G, Mazoyer B, Tzourio-Mazoyer N (2006) Handedness and cerebral anatomical asymmetries in young adult males. *Neuroimage* 29:1066–1079.
- Holloway RL (1988) Some additional morphological and metrical observations on *Pan* brain casts and their relevance to the Taung endocast. *Am J Phys Anthropol* 77:27–33.
- Holloway RL, Broadfield DC, Yuan MS (2001) Revisiting Australopithecine visual striate cortex: Newer data from chimpanzee and human brains suggest it could have been reduced during Australopithecine times. *Evolutionary Anatomy of the Primate Cerebral Cortex*, eds Falk D, Gibbon K (Cambridge Univ Press, Cambridge, UK), pp 177–186.
- Kubo D, Kono RT, Kaifu Y (2013) Brain size of *Homo floresiensis* and its evolutionary implications. *Proc Biol Sci* 280:20130338.
- Spoor F, et al. (2015) Reconstructed *Homo habilis* type OH 7 suggests deep-rooted species diversity in early *Homo*. *Nature* 519:83–86.
- Holloway RL, Broadfield DC, Yuan MS (2004) Brain endocasts the paleoneurological evidence. *The Human Fossil Record* (Wiley-Liss, New York), Vol 3.
- Lordkipanidze D, et al. (2013) A complete skull from Dmanisi, Georgia, and the evolutionary biology of early *Homo*. *Science* 342:326–331.
- Stout D, Toth N, Schick K, Chaminade T (2008) Neural correlates of Early Stone Age toolmaking: Technology, language and cognition in human evolution. *Philos Trans R Soc Lond B Biol Sci* 363:1939–1949.
- Putt SS, Wijekumar S, Franciscus RG, Spencer JP (2017) The functional brain networks that underlie Early Stone Age tool manufacture. *Nat Hum Behav* 1:0102.
- Schoenemann PT, Holloway RL (2016) Brain function and Broca's Cap: A meta-analysis of fMRI studies. *Am J Phys Anthropol* 159:283.

